



Synthesis and Anti-Trypanosoma cruzi Biological Evaluation of Novel 2-Nitropyrrole Derivatives

Fanny Mathias, Youssef Kabri, Damien Brun, Nicolas Primas, Carole Di Giorgio, Patrice Vanelle

► To cite this version:

Fanny Mathias, Youssef Kabri, Damien Brun, Nicolas Primas, Carole Di Giorgio, et al.. Synthesis and Anti-Trypanosoma cruzi Biological Evaluation of Novel 2-Nitropyrrole Derivatives. *Molecules*, 2022, 27 (7), pp.2163. 10.3390/molecules27072163 . hal-03818628

HAL Id: hal-03818628

<https://amu.hal.science/hal-03818628>

Submitted on 18 Oct 2022

HAL is a multi-disciplinary open access archive for the deposit and dissemination of scientific research documents, whether they are published or not. The documents may come from teaching and research institutions in France or abroad, or from public or private research centers.

L'archive ouverte pluridisciplinaire **HAL**, est destinée au dépôt et à la diffusion de documents scientifiques de niveau recherche, publiés ou non, émanant des établissements d'enseignement et de recherche français ou étrangers, des laboratoires publics ou privés.



Distributed under a Creative Commons Attribution| 4.0 International License

Synthesis and Anti-*Trypanosoma cruzi* Biological Evaluation of Novel 2-Nitropyrrole Derivatives

Fanny Mathias ^{1,2}, Youssef Kabri ¹, Damien Brun ¹, Nicolas Primas ^{1,3} , Carole Di Giorgio ⁴ and Patrice Vanelle ^{1,3,*}

¹ Equipe Pharmaco-Chimie Radicalaire, CNRS, ICR UMR 7273, Faculté de Pharmacie, Aix Marseille University, 27 Boulevard Jean Moulin, CS30064, CEDEX 05, 13385 Marseille, France; fanny.mathias@univ-amu.fr (F.M.); youssef.kabri@univ-amu.fr (Y.K.); brundamien83@gmail.com (D.B.); nicolas.primas@univ-amu.fr (N.P.)

² Assistance Publique-Hôpitaux de Marseille (APHM), Pharmacie Usage Intérieur, Hôpital Nord, Chemin-des-Bourrely, 13015 Marseille, France

³ Assistance Publique-Hôpitaux de Marseille (APHM), Service Central de la Qualité et de l'Information Pharmaceutiques (SCQIP), Hôpital de la Conception, 147, Boulevard Baille, 13005 Marseille, France

⁴ Laboratoire de Mutagénèse Environnementale, CNRS, IRD, Aix Marseille University, IMBE UMR 7263, Avignon University, 13385 Marseille, France; carole.di-giorgio@univ-amu.fr

* Correspondence: patrice.vanelle@univ-amu.fr; Tel.: +33-4-9183-5580

Abstract: Human American trypanosomiasis, called Chagas disease, caused by *T. cruzi* protozoan infection, represents a major public health problem, with about 7000 annual deaths in Latin America. As part of the search for new and safe anti-*Trypanosoma cruzi* derivatives involving nitroheterocycles, we report herein the synthesis of ten 1-substituted 2-nitropyrrole compounds and their biological evaluation. After an optimization phase, a convergent synthesis methodology was used to obtain these new final compounds in two steps from the 2-nitropyrrole starting product. All the designed derivatives follow Lipinski's rule of five. The cytotoxicity evaluation on CHO cells showed no significant cytotoxicity, except for compound **3** (CC₅₀ = 24.3 μM). Compound **18** appeared to show activity against *T. cruzi* intracellular amastigotes form (EC₅₀ = 3.6 ± 1.8 μM) and good selectivity over the vero host cells. Unfortunately, this compound **18** showed an insufficient maximum effect compared to the reference drug (nifurtimox). Whether longer duration treatments may eliminate all parasites remains to be explored.

Keywords: chagas disease; *T. cruzi*; pyrrole; nitro-heterocycle

1. Introduction

Trypanosoma cruzi is a flagellate protozoan involved in Chagas disease (Human American trypanosomiasis), a neglected tropical disease causing a major public health problem, with about 7000 annual deaths in Latin America [1]. Although asymptomatic in the acute phase after contamination, cardiac and digestive complications may appear in 20 to 30% of cases during the chronic phase of the disease (inflammatory cardiomyopathy, enlargement of the gastrointestinal tract and organs, and gastrointestinal motor disorders) [2,3].

The anti-trypanosomatid potential of nitroheterocycles is well known, such as benznidazole (2-nitroimidazole) and nifurtimox (5-nitrofuran) listed on the WHO Model list of essential medicines for the treatment of human American trypanosomiasis (Figure 1) [4]. These two compounds represent an important part of the therapeutic arsenal in the management of Chagas disease. However, they are active mainly in the acute and early chronic stage of the disease, but not once in the late stage [5]. Their use is also limited by their toxicity, making the development of new safe and effective drugs against *T. cruzi* necessary. Recently, an orally available 5-nitroimidazole, fexinidazole, was identified as a promising new drug candidate for the treatment of both stages of human African trypanosomiasis due to *Trypanosoma brucei gambiense* infection [6]. The clinical evaluation of this compound on

the treatment of adults with chronic indeterminate Chagas disease due to *T. cruzi* infection is in progress [7,8].

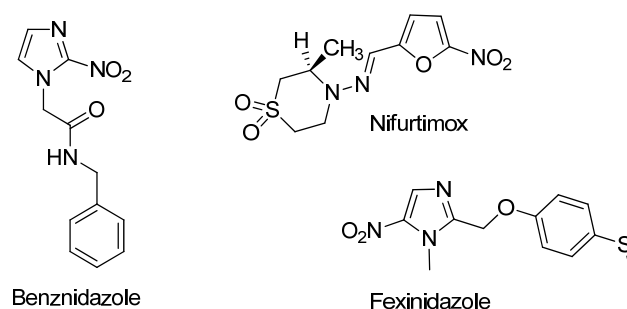


Figure 1. Nitroheterocycles marketed for the management of trypanosomiasis.

On the other hand, several research studies were carried out on heterocyclic nitrogen mono-cyclic (imidazole, thiazole, triazole) or bicyclic (benzimidazole, imidazopyridine, imidazooxazole, imidazooxazine) series with several mechanisms of action identified against *T. cruzi* [9–12]. Only a few recent publications have shown that pyrrole derivatives could have good anti-*Trypanosoma cruzi* activity by inhibition of an enzyme involved in the synthesis of sterols, 14 α -demethylase, also known as CYP51 [13].

The aim of this work was to synthesize 2-nitropyrrole derivatives functionalized at the N1-position by a chain structurally close to that found in benznidazole (Figure 2). Several nitro-drugs are known to act as prodrugs bioactivated by *T. cruzi* nitro-reductases NTR type I [14,15], capable of exerting cytotoxic effects via DNA damage. We will investigate whether the synthesized 2-nitropyrrole derivatives exhibit anti-*T. cruzi* activity.

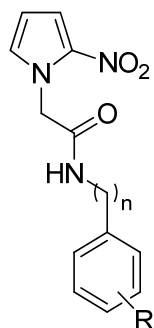
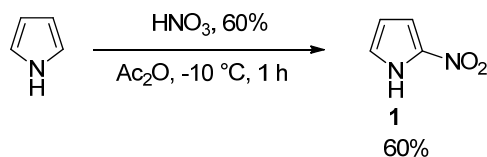


Figure 2. General structure of 2-nitropyrrole derivatives synthesized.

2. Results and Discussion

2.1. Chemistry

The regioselective nitration of the commercial pyrrole using previous report allows us to synthesize 2-nitropyrrole starting product in 60% yield (Scheme 1) [16].



Scheme 1. Synthesis of 2-nitropyrrole starting product 1.

The X-ray crystal structure (Figure 3) was determined for this compound to confirm the regioselective nitration reaction at the 2-position of the pyrrole compound (CCDC 2132900).

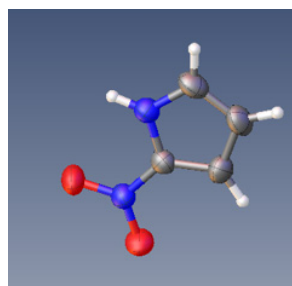


Figure 3. X-ray crystal structure of 2-nitropyrrole starting product **1**.

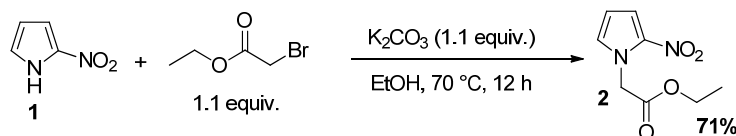
The pyrrole nitration must be carried out under mild conditions using acetic anhydride as a solvent, because in the presence of sulfuric acid, only the polymerization of the pyrrole was reported, without the formation of the target product [17].

In the reaction conditions described in Scheme 1, we observed the formation of the expected product (**1**) in good yield, traces of the dinitro pyrrole product observed by LC/MS monitoring but not isolated, as well as a black resin which may correspond to a polymerization side-product, as reported in the literature [17].

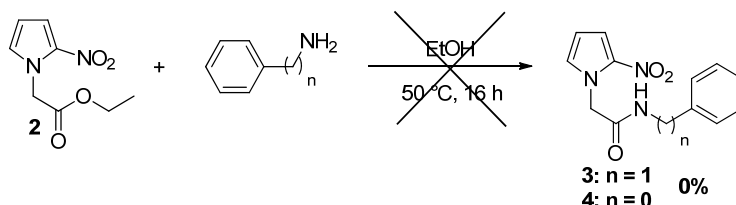
Then, we tried two alkylation protocols to obtain the 2-nitropyrrole derivatives functionalized at position N-1.

First, we applied the benznidazole alkylation protocol on the 2-nitropyrrole starting product in two steps (Scheme 2) [18].

Step 1:



Step 2:



Scheme 2. Alkylation using the benznidazole alkylation protocol in two steps.

The first alkylation step with ethyl bromoacetate led to the desired compound **2** in a 71% yield (Scheme 2, step 1). Unfortunately, the second amidification step with benzylamine and aniline did not lead to the desired compounds **3** or **4** (Scheme 2, step 2). LC/MS monitoring of this reaction revealed the disappearance of the starting product signal and the absence of formation of the desired products **3** or **4**. A reaction optimization using LC/MS monitoring was therefore conducted by varying different parameters according to amidification protocols described in the literature (Table 1) [19]. The various attempts were not conclusive, and we never observed the expected product **3** or **4** by LC/MS monitoring. The formation of a black resin was visually observed for attempts 1, 4 and 5. It was described in the literature that the reactions on pyrrole consuming the starting product, without the formation of the desired product or other side products, suggested a pyrrole polymerization because of its high reactivity [17].

In the first step, we showed that the pyrrole alkylation with ethyl bromoacetate was successfully conducted (Scheme 2, step 1). The limiting step was the amidification reaction. We have therefore changed the procedure and decided to use a convergent synthesis methodology: performing, on one hand, the acylation of various primary amine to form

bromoacetamide intermediates and carry out the substitution reaction on the pyrrole **1** in the last step. The acylation of commercially available 2-bromoacetyl bromide was successfully carried out with 10 different amines using the experimental protocol reported in the literature (Table 2) [20].

Table 1. Optimization of the amidification reaction on compound **2**.

Entry	Amine	Base	Temp (°C)	Time (h)	Solvent	2 (%)	3 (%)	4 (%)
1	Benzylamine	K ₂ CO ₃	50	24	EtOH	0	0	-
2	Benzylamine	-	50	48	EtOH	100	0	-
3	Phenylamine	-	80	48	EtOH	100	-	0
4 ^a	Phenylamine	NaH	rt	24	DMSO	0	-	0
5 ^b	Phenylamine	DMAP	150	1	Toluene	0	-	0

^a: reaction under inert atmosphere (N₂); ^b: reaction under microwave irradiation.

Table 2. Synthesis of bromoacetamide intermediate compounds.

$\text{Br}-\text{C}(=\text{O})-\text{CH}_2-\text{Br} + \text{R}-\text{NH}_2 \xrightarrow[\text{CH}_2\text{Cl}_2, 0^\circ\text{C}, 12\text{ h}]{\text{Et}_3\text{N (1 equiv.)}} \text{R}-\text{NH}-\text{C}(=\text{O})-\text{CH}_2-\text{Br}$ <p style="text-align: center;">1 equiv.</p>		
Compound	Structure	Yield (%)
5		82
6		99
7		18
8		91
9		44
10		48
11		46
12		25
13		87
14		25

Secondly, we performed a nucleophilic substitution reaction between compound **1** and bromoacetamide intermediates (**5–14**) to obtain the 2-nitropyrrole derivatives functionalized in 1-position (Table 3). This synthetic methodology was applied to the various bromoacetamide intermediates **5** to **14** to obtain final compounds **3–4** and **15–22** in good yields ranging from 58% to 96%, except for compound **20** obtained in a lower yield of 30%. Under these conditions, we did not observe any problem related to the polymerization of pyrrole.

Table 3. Synthesis of 2-nitropyrrole derivatives functionalized at position 1 (**3–4**, **15–22**).

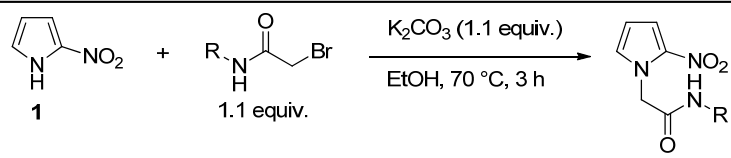
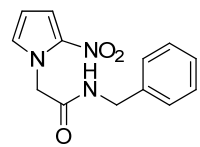
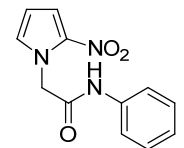
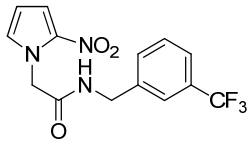
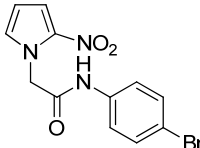
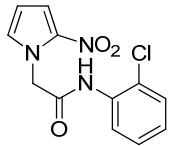
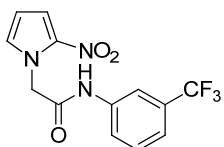
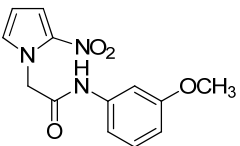
<div style="text-align: center;">  </div>		
Compounds 5–14		Compounds 3–4 , 15–22
Compound	Structure	Yield (%)
3		73
4		78
15		60
16		86
17		96
18		81
19		88

Table 3. Cont.

<div style="display: flex; justify-content: space-around;"> <div> <p>1</p> </div> <div> <p>Compounds 5-14</p> </div> <div> <p>Compounds 3-4, 15-22</p> </div> </div>		
Compound	Structure	Yield (%)
20		30
21		59
22		77

2.2. Biological Evaluation

2.2.1. Cytotoxicity and anti-*T. cruzi* Biological Evaluation

These new derivatives were evaluated *in vitro* against the intracellular *T. cruzi* strain X10/7-Silvio by determining their 50% efficacy concentration (EC₅₀) and were compared to the reference anti-*T. cruzi* drug nifurtimox. The *in vitro* 50% cytotoxic concentrations (CC₅₀) were assessed on the CHO cell line and compared to a cytotoxic reference drug, doxorubicin. *In vitro* cytotoxicity against vero host cells was also assessed (vero cells EC₅₀). The results are presented in Table 4.

Regarding the effect on cell viability of the CHO cells, except for one compound (3), the other derivatives showed good cytotoxicity values ranging from 155.6 to 321.1 µM compared to the reference drug, doxorubicin (CC₅₀ CHO = 4.6 µM). Three compounds showed no cytotoxicity against vero host cells at concentrations up to 50 µM (17–19).

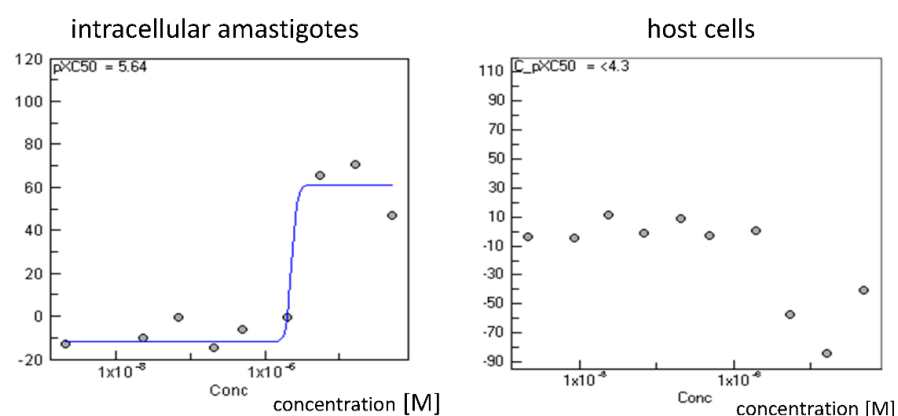
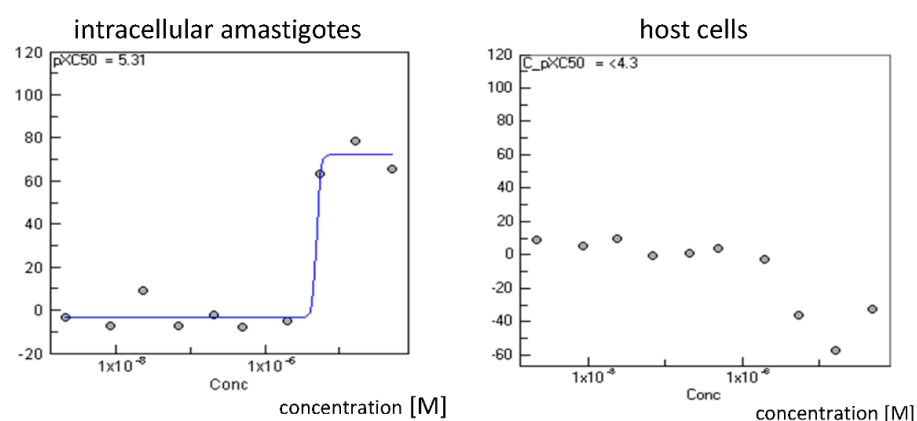
Of the 10 synthesized molecules, three showed poor DMSO solubility, limiting their *in vitro* anti-*T. cruzi* evaluation (20–22). Three compounds showed *T. cruzi* EC₅₀ < 10 µM (4, 16 and 18). Only compound 18 exhibited activity against the parasite (EC₅₀ = 3.6 ± 1.8 µM) without toxicity against host cells at concentrations up to 50 µM. However, the maximum effect of the latter compound (Figure 4) compared to the nifurtimox control (Figure 5) was relatively low (79% and 71% in two independent replicates), indicating that a substantial number of parasites survive 96h treatment. Whether longer duration treatments may eliminate all parasites remains to be explored.

The structure–activity relationship (SAR) can be suggested from these biological results. The presence of a benzyl group seems to be unfavourable for anti-*T. cruzi* activity. Indeed, compounds 3 and 15 with respectively benzyl and *meta*-EWG 3-CF₃ benzyl group exhibit no activity against *T. cruzi* (EC₅₀ = 34.5 µM and 41.0 µM), whereas their analogue with phenyl (4) and *meta*-EWG 3-CF₃ phenyl group (18) exhibits activity (EC₅₀ < 10 µM). The *meta*-EWG 3-CF₃ phenyl group gave the best anti-*T. cruzi* activity (18), while the *meta*-electro-donating OCH₃ phenyl group (19) gave the lowest anti-*T. cruzi* activity (EC₅₀ = 50.0 µM). An electron-withdrawing (EWG) group in the *meta*-position of the phenyl seems to be important for anti-*T. cruzi* activity.

Table 4. Activity and cytotoxicity evaluation of 2-nitropyrrole derivatives.

Compound	Activity	Toxicity	
	EC ₅₀ <i>T. cruzi</i> (μM) ^a	Vero cells EC ₅₀ (μM)	CC ₅₀ CHO (μM) ^b
3	34.5 ± 21.9	42 ± 11.3	24.2 ± 1.2
4	6.0	14.0	262.1 ± 3.9
15	41.0 ± 12.7	43 ± 9.9	184.9 ± 5.1
16	6.5 ± 0.6	14.5 ± 0.7	173.0 ± 4.6
17	50.0	>50	198.3 ± 5.7
18	3.6 ± 1.8	>50	155.6 ± 2.9
19	50.0	>50	260.1 ± 6.3
20	-	-	321.1 ± 5.3
21	-	-	303.3 ± 6.1
22	-	-	188.2 ± 4.4
Doxorubicin	-	-	4.6 ± 0.08
Nifurtimox	2.1 ± 0.2	-	-

^a Results are the mean ± SD of two independent biological replicates. ^b Results are the mean ± SD of three independent biological replicates.

Replicate 1**Replicate 2****Figure 4.** Dose response curves for compound 18 against *T. cruzi* X10/7 intracellular amastigotes. Left panels show percent inhibition of intracellular amastigotes (normalised to DMSO (0%) and nifurtimox controls (100%)). Right-hand panels show inhibition of Vero host cell growth. The negative inhibition of Vero cells at concentrations that inhibit parasite growth reflect the absence of host cell lysis due to parasite egress, which is seen in the DMSO control. Replicates are from separate experiments.

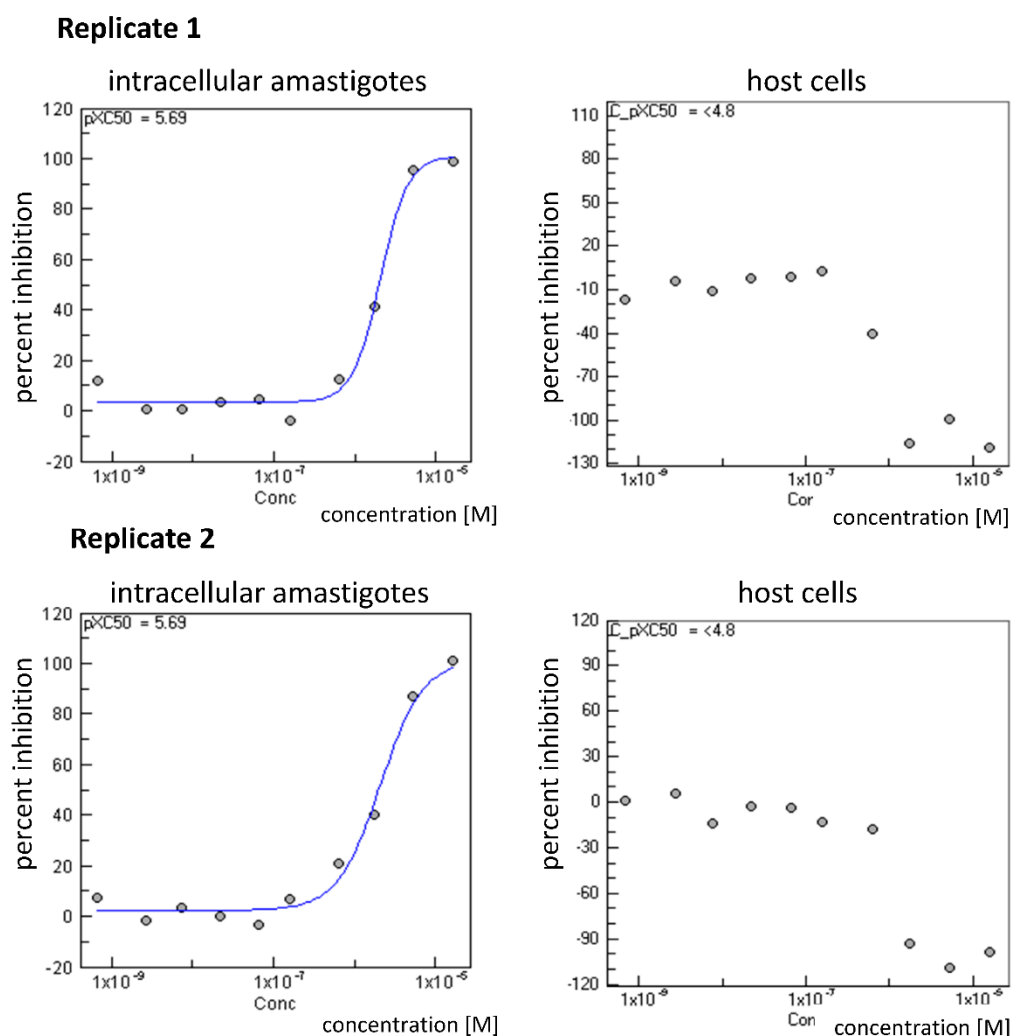


Figure 5. Dose response curves for nifurtimox against *T. cruzi* X10/7 intracellular amastigotes. Left panels show percentage inhibition of intracellular amastigotes (normalised to DMSO (0%) and nifurtimox controls (100%)). Right-hand panels show the inhibition of Vero host cell growth. The negative inhibition of Vero cells at concentrations that inhibit parasite growth reflects the absence of host cell lysis due to parasite egress, which is seen in the DMSO control. Replicates are from separate experiments.

2.2.2. In Silico ADME Properties

The ADME properties of 2-nitropyrrole derivatives (3–4, 15–22) were predicted by using molinspiration [21]. The designed derivatives follow Lipinski's rule of five (Table 5) [22]. There are less than 5 H-bond donors, the molecular weight is less than 500 g·mol⁻¹, the logP is less than 5, and there are less than 10 H-bond acceptors. In addition, the TPSA was <140 Å² (Veber's rules). There are no parameters out of range, so we did not identify any alerts of poor absorption or permeability for the oral route of administration.

Compliance with Lipinski's rule of five is reassuring, but we must keep in mind that not all drugs fully comply with this rule, especially in the antimicrobial field [23].

Table 5. Predicted Lipinski parameters and ADME properties.

Compound	XlogP (o/w)	Mol. Wt. (g·mol ⁻¹)	HBA	HDA	nrotb	TPSA (Å ²)
3	1.51	259.26	6	1	5	79.86
4	1.81	245.24	6	1	4	79.86
15	2.38	327.26	6	1	6	79.86
16	2.62	324.13	6	1	4	79.86
17	2.44	279.68	6	1	4	79.86
18	2.65	313.24	6	1	5	79.86
19	1.84	275.26	7	1	5	89.09
20	0.78	211.22	6	1	4	79.86
21	1.51	237.26	6	1	4	79.86
22	2.71	342.12	6	1	4	79.86

HBA: Number of hydrogen-bond acceptors (O and N atoms); HDA: Number of hydrogen-bond donors (OH and NH groups); nrotb: no of rotatable bonds; XlogP (o/w): Octanol-water partition coefficient; TPSA: Topological polar surface area.

3. Materials and Methods

3.1. Chemistry

3.1.1. Generality

Melting points were determined on a Köfler melting point apparatus (Wagner & Munz GmbH, München, Germany) and were uncorrected. NMR spectra were recorded on AV 250 spectrometers or a Bruker Avance NEO 400 MHz NanoBay spectrometer at the Faculté de Pharmacie of Marseille or on a Bruker Avance III nanobay 400 MHz spectrometer at the Spectropole, Faculté des Sciences de Saint-Jérôme (Marseille). (¹H NMR: reference CHCl₃ δ = 7.26 ppm, reference DMSO-d₆ δ = 2.50 ppm and ¹³C NMR: reference CHCl₃ δ = 76.9 ppm, reference DMSO-d₆ δ = 39.52 ppm). The following adsorbent was used for column chromatography: silica gel 60 (Merck KGaA, Darmstadt, Germany, particle size 0.063–0.200 mm, 70–230 mesh ASTM). TLC was performed on 5 cm × 10 cm aluminium plates coated with silica gel 60F-254 (Merck) in an appropriate eluent. Visualisation was performed with ultraviolet light (254 nm). The purity of synthesised compounds was checked by LC/MS analyses, which were realized at the Faculté de Pharmacie of Marseille with a Thermo Scientific Accela High Speed LC System[®] (Waltham, MA, USA) coupled using a single quadrupole mass spectrometer Thermo MSQ Plus[®]. The RP-HPLC column is a Thermo Hypersil Gold[®] 50 × 2.1 mm (C18 bounded), with particles of a diameter of 1.9 µm. The volume of sample injected on the column was 1 µL. Chromatographic analysis, total duration of 8 min, was on the gradient of the following solvents: t = 0 min, methanol/water 50:50; 0 < t < 4 min, linear increase in the proportion of methanol to a methanol/water ratio of 95:5; 4 < t < 6 min, methanol/water 95:5; 6 < t < 7 min, linear decrease in the proportion of methanol to return to a methanol/water ratio of 50:50; 6 < t < 7 min, methanol/water 50:50. The water used was buffered with ammonium acetate 5 mM. The flow rate of the mobile phase was 0.3 mL/min. The retention times (t_R) of the molecules analysed were indicated in min. High-resolution MS experiments were performed at the Spectropole (Campus Etoile, Aix-Marseille Université, France) with a SYNAPT G2 HDMS quadrupole/time-of-flight (Q/ToF) (Waters, Manchester, UK) using the following parameters: ESI capillary voltage: +2.8 kV; extraction cone voltage: 20 V; and desolvation gas flow rate (nitrogen): 100 L·h⁻¹. The accurate mass measurements were carried out in triplicate with an external calibration. Reagents were purchased and used without further purifications from Sigma-Aldrich or Fluorochem. The starting product 2-nitropyrrole (1) was prepared using previous reports [16]. Please see Supplementary Materials for details.

3.1.2. Synthesis of Ethyl 2-(2-nitro-1H-pyrrol-1-yl)acetate (2)

To a solution of 2-nitropyrrole (0.5 g, 4.76 mmol) in EtOH (20 mL) was added K₂CO₃ (0.679 g, 4.91 mmol, 1.1 eq) and ethyl bromoacetate (0.544 mL, 4.91 mmol, 1.1 eq). The reaction mixture was heated at 70 °C for 12 h. After EtOH evaporation, 20 mL of water was poured on the crude product and the aqueous layer was extracted with dichloromethane (3 × 50 mL). The organic layer was washed with brine (3 × 100 mL), dried over Na₂SO₄, and evaporated. The crude product was purified by column chromatography (silica gel, petroleum ether/ethyl acetate 9:1).

Yield 71% (629 mg). White solid. Mp 51–52 °C. ¹H NMR (400 MHz, CDCl₃) δ 7.26–7.24 (m, 1H, CH), 6.81 (dd, ³J_{H-H} = 2.8 Hz, ⁴J_{H-H} = 2.1 Hz, 1H, CH), 6.25 (dd, ³J_{H-H} = 4.4 Hz, ⁴J_{H-H} = 2.8 Hz, 1H, CH), 5.02 (s, 2H, CH₂), 4.24 (q, ³J_{H-H} = 7.1 Hz, 2H, CH₂), 1.28 (t, ³J_{H-H} = 7.1 Hz, 3H, CH₃). ¹³C NMR (100 MHz, CDCl₃) δ 167.5 (C), 137.7 (C), 130.0 (CH), 114.9 (CH), 109.2 (CH), 62.2 (CH₂), 51.7 (CH₂), 14.2 (CH₃).

3.1.3. General Procedure for the Synthesis of Bromoacetamide Intermediate Derivatives

In a first vial, dichloromethane (10 mL) was added to bromoacetyl bromide (216 µL, 2.48 mmol, 1 eq). In a second vial, dichloromethane (10 mL) was added to the corresponding amine (2.48 mmol, 1 eq) and Et₃N (345 µL, 2.48 mmol, 1 eq). The two reactions mixtures were respectively stirred for 5 min at 0 °C in a bath of ice. The second solution mixture was added dropwise at 0 °C to the first bromoacetyl bromide solution, and the reaction mixture was stirred from 0 °C to room temperature for 12 h. The solution was poured into a bath of ice. The aqueous layer was extracted with dichloromethane (3 × 100 mL) and the organic layer was washed with brine (3 × 100 mL), dried over Na₂SO₄, and evaporated. Intermediate compounds were obtained without purification, except for compounds 7, 10, 11, 14.

N-Benzyl-2-bromoacetamide (5) [24]

Yield 82% (460 mg). White solid. Lit. Mp 106–107.5 °C [25]. ¹H NMR (400 MHz, DMSO-*d*₆) δ 8.78 (s, 1H, NH), 7.35–7.31 (m, 2H, 2CH), 7.27–7.25 (m, 3H, 3CH), 4.30 (d, ³J_{H-H} = 6.0 Hz, 2H, CH₂), 3.91 (s, 2H, CH₂). The ¹H NMR data were in agreement with the literature values. Lit. ¹³C NMR (125 MHz, CDCl₃) δ 165.3 (C), 137.2 (C), 128.8 (2CH), 127.8 (CH), 127.7 (2CH), 44.2 (CH₂), 29.1 (CH₂).

2-Bromo-*N*-phenylacetamide (6) [24,26]

Yield 99% (525 mg). Brown solid. Lit. Mp 129–131 °C (isopropyl ether) [26]. ¹H NMR (400 MHz, DMSO-*d*₆) δ 10.37 (s, 1H, NH), 7.60–7.57 (m, 2H, 2CH), 7.35–7.30 (m, 2H, 2CH), 7.10–7.07 (m, 1H, CH), 4.04 (s, 2H, CH₂). The ¹H NMR data were in agreement with the literature values. Lit. ¹³C NMR (125 MHz, CDCl₃) δ 163.3 (C), 136.9 (C), 129.1 (2CH), 125.2 (2CH), 120.0 (CH), 29.5 (CH₂).

2-Bromo-*N*-[3-(trifluoromethyl)benzyl]acetamide (7) [27]

The crude product was purified by column chromatography (silica gel, dichloromethane/petroleum ether from 2/8 to 8/2). Yield 18% (130 mg). Brown solid. Lit. Mp 251–253 °C [28]. ¹H NMR (400 MHz, CDCl₃) δ 7.57–7.53 (m, 2H, 2CH), 7.49–7.47 (m, 2H, 2CH), 6.86 (s, 1H, NH), 4.54 (d, ³J_{H-H} = 6.1 Hz, 2H, CH₂), 3.95 (s, 2H, CH₂). The ¹H NMR data were in agreement with the literature values. Lit. ¹³C NMR (CDCl₃, 75 MHz) δ 165.6 (C), 141.4 (C), 130.0 (q, ³J_{C-F} = 32.3 Hz, C), 127.8 (2CH), 125.7 (q, ⁴J_{C-F} = 3.8 Hz, CH), 122.1 (CH), 118.6 (C), 43.6 (CH₂), 28.9 (CH₂).

2-Bromo-*N*-(4-bromophenyl)acetamide (8) [29]

Yield 91% (657 mg). Brown solid. Lit. Mp 148–150 °C. ¹H NMR (400 MHz, DMSO-*d*₆) δ 10.51 (s, 1H, NH), 7.57–7.50 (m, 4H, 4CH), 4.03 (s, 2H, CH₂). The ¹H NMR data were in agreement with the literature values. Lit. ¹³C NMR (CDCl₃, 100 MHz,) δ 163.3 (C), 136.0 (C), 132.1 (2CH), 121.5 (2CH), 117.9 (C), 29.3 (CH₂).

2-Bromo-*N*-(2-chlorophenyl)acetamide (9)

Yield 44% (657 mg). Brown solid. Mp 92–93 °C. ¹H NMR (400 MHz, DMSO-d₆) δ 9.94 (s, 1H, NH), 7.71 (dd, ³J_{H-H} = 6.1 Hz, ⁴J_{H-H} = 1.7 Hz, 1H, CH), 7.52 (dd, ³J_{H-H} = 8.0 Hz, ⁴J_{H-H} = 1.5 Hz, 1H, CH), 7.35 (td, ³J_{H-H} = 7.8 Hz, ⁴J_{H-H} = 1.5 Hz, 1H, CH), 7.23 (td, ³J_{H-H} = 7.7 Hz, ⁴J_{H-H} = 1.7 Hz, 1H, CH), 4.17 (s, 2H, CH₂). The ¹H NMR data were in agreement with the literature values. ¹³C NMR (100 MHz, DMSO-d₆) δ 170.7 (C), 134.2 (C), 129.3 (CH), 127.9 (2CH), 125.3 (CH), 122.0 (C), 61.6 (CH₂).

2-Bromo-N-[3-(trifluoromethyl)phenyl]acetamide (**10**) [28]

The crude product was purified by column chromatography (silica gel, dichloromethane/petroleum ether 6/4). Yield 48% (331 mg). White solid. Lit. Mp 78–81 °C. ¹H NMR (400 MHz, DMSO-d₆) δ 10.72 (s, 1H, NH), 8.07 (s, 1H, CH), 7.76 (d, ³J_{H-H} = 8.4 Hz, 1H, CH), 7.60–7.56 (m, 1H, CH), 7.44 (d, ³J_{H-H} = 7.6 Hz, 1H, CH), 4.07 (s, 2H, CH₂). The ¹H NMR data were in agreement with the literature values. Lit. ¹³C NMR (100 MHz, CDCl₃): δ 173.7 (C), 138.4 (C), 130.9 (C), 130.6 (CH), 127.8 (CH), 124.6 (C), 123.5 (CH), 123.1 (CH), 42.7 (CH₂).

2-Bromo-N-(3-methoxyphenyl)acetamide (**11**) [30]

The crude product was purified by column chromatography (silica gel, dichloromethane/petroleum ether 6/4). Yield 46% (280 mg). White solid. Mp 94–95 °C. ¹H NMR (400 MHz, CDCl₃) δ 8.10 (s, 1H, NH), 7.27–7.26 (m, 1H, CH), 7.25–7.23 (m, 1H, CH), 7.02–6.99 (m, 1H, CH), 6.73–6.71 (m, 1H, CH), 4.02 (s, 2H, CH₂), 3.81 (s, 3H, CH₃). The ¹H NMR data were in agreement with the literature values. Lit. ¹³C NMR (63 MHz, DMSO-d₆) δ 164.7 (C), 159.5 (C), 139.7 (C), 129.6 (CH), 111.5 (CH), 109.2 (CH), 105.0 (CH), 55.0 (CH₃), 30.4 (CH₂).

2-Bromo-N-isopropylacetamide (**12**) [31]

Yield 25% (100 mg). White solid. Mp Lit. 63–64 °C. ¹H NMR (400 MHz, CDCl₃) δ 6.29 (s, 1H, NH), 4.10–4.02 (m, 1H, CH), 3.85 (s, 2H, CH₂), 1.19 (d, ³J_{H-H} = 6.5 Hz, 6H, 2CH₃). The ¹H NMR data were in agreement with the literature values. Lit. ¹³C NMR (400 MHz, CDCl₃) δ 164.4 (C), 42.3 (CH), 29.4 (CH₂), 22.4 (2CH₃).

2-Bromo-N-cyclopentylacetamide (**13**) [31]

Yield 87% (443 mg). White solid. Mp Lit. 84–85 °C. ¹H NMR (400 MHz, CDCl₃) δ = 6.74 (s, 1H, NH), 4.13–4.08 (m, 1H, CH), 3.78 (s, 2H, CH₂), 1.94–1.87 (m, 2H, CH₂), 1.65–1.63 (m, 2H, CH₂), 1.56–1.53 (m, 2H, CH₂), 1.40–1.36 (m, 2H, CH₂). The ¹H NMR data were in agreement with the literature values. Lit. ¹³C NMR (400 MHz, CDCl₃) δ = 164.8 (C), 51.8 (CH), 32.8 (2CH₂), 29.4 (CH₂), 23.6 (2CH₂).

2-Bromo-N-(2-bromo-5-fluorophenyl)acetamide (**14**)

The crude product was purified by column chromatography (silica gel, dichloromethane/petroleum ether 5/5). Yield 25% (280 mg). White solid. Mp. 99–100 °C. ¹H NMR (400 MHz, CDCl₃) δ 8.86 (s, 1H, NH), 8.24–8.21 (m, 1H, CH), 7.53–7.50 (m, 1H, CH), 6.81–6.76 (m, 1H, CH), 4.08 (s, 2H, CH₂). ¹³C NMR (100 MHz, CDCl₃) δ 163.7 (C), 162.1 (d, ¹J_{C-F} = 246.3 Hz, C), 136.3 (d, ³J_{C-F} = 11.6 Hz, C), 133.1 (d, ³J_{C-F} = 9.5 Hz, CH), 113.0 (d, ²J_{C-F} = 23.2 Hz, CH), 108.9 (d, ²J_{C-F} = 29.1 Hz, CH), 107.7 (d, ⁴J_{C-F} = 3.6 Hz, C), 29.7 (CH₂).

3.1.4. General Procedure for the Synthesis of 2-Nitropyrrole Derivatives

To a solution of 2-nitropyrrole (0.1 g, 0.9 mmol, 1 eq) in ethanol (5 mL) was added K₂CO₃ (0.138 g, 0.99 mmol, 1.1 eq), and the corresponding bromoacetamide compound (1.1 eq). The reaction mixture was stirred and heated at 70 °C for 3 h. After cooling, the solution was poured into a bath of ice. A precipitate appeared and was filtered, washed with water (3 × 100 mL), petroleum ether (3 × 100 mL), and dried in a vacuum drying oven (desiccator cabinet).

N-Benzyl-2-(2-nitro-1H-pyrrol-1-yl)acetamide (**3**)

Yield 73% (113 mg). White solid. Mp 174–175 °C. ¹H NMR (400 MHz, DMSO-*d*₆) δ 8.70 (s, 1H, NH), 7.33–7.25 (m, 7H, 7CH), 6.28 (dd, $3J_{\text{H-H}} = 4.4$ Hz, $4J_{\text{H-H}} = 2.7$ Hz, 1H, CH), 5.09 (s, 2H, CH₂), 4.32 (d, $3J_{\text{H-H}} = 5.9$ Hz, 2H, CH₂). ¹³C NMR (100 MHz, DMSO-*d*₆) δ 167.1 (C), 139.5 (C), 137.6 (C), 132.9 (CH), 128.7 (2CH), 127.7 (2CH), 127.3 (CH), 114.8 (CH), 109 (CH), 52.6 (CH₂), 42.7 (CH₂). LC-MS (ESI+) Tr 4.12 min, m/z [M + H]⁺ 260.18. MW: 259.10 g·mol⁻¹. HRMS: m/z [M + H]⁺ calcd for [C₁₃H₁₃N₃O₃]⁺: 260.1030; found: 260.1029.

2-(2-Nitro-1*H*-pyrrol-1-yl)-*N*-phenylacetamide (4)

Yield 78% (170 mg). White solid. Mp 201–202 °C. ¹H NMR (400 MHz, DMSO-*d*₆) δ 10.4 (s, 1H, NH), 7.57–7.55 (m, 2H, 2CH), 7.36–7.28 (m, 4H, 4CH), 7.06 (t, $3J_{\text{H-H}} = 7.4$ Hz, 1H, CH), 6.32 (dd, $3J_{\text{H-H}} = 4.4$ Hz, $4J_{\text{H-H}} = 2.7$ Hz, 1H, CH), 5.24 (s, 2H, CH₂). ¹³C NMR (100 MHz, DMSO-*d*₆) δ 165.3 (C), 138.7 (C), 137.0 (C), 132.5 (CH), 128.9 (2CH), 123.5 (CH), 119.0 (2CH), 114.4 (CH), 108.6 (CH), 52.8 (CH₂). LC-MS (ESI+) Tr 4.08 min, m/z [M + H]⁺ 246.21. MW: 245.08 g·mol⁻¹. HRMS: m/z [M + H]⁺ calcd for [C₁₂H₁₁N₃O₃]⁺: 246.0873; found: 246.0873.

2-(2-Nitro-1*H*-pyrrol-1-yl)-*N*-[3-(trifluoromethyl)benzyl]acetamide (15)

Yield 60% (172 mg). White solid. Mp 161–162 °C. ¹H NMR (400 MHz, DMSO-*d*₆) δ 8.81 (s, 1H, NH), 7.64–7.57 (m, 4H, 4CH), 7.33–7.30 (m, 1H, CH), 7.25 (dd, $3J_{\text{H-H}} = 4.1$ Hz, $4J_{\text{H-H}} = 1.9$ Hz, 1H, CH), 6.28 (dd, $3J_{\text{H-H}} = 3.8$ Hz, $4J_{\text{H-H}} = 2.7$ Hz, 1H, CH), 5.11 (s, 2H, CH₂), 4.42 (d, $3J_{\text{H-H}} = 5.8$ Hz, 2H, CH₂). ¹³C NMR (100 MHz, DMSO-*d*₆) δ 167.0 (C), 140.7 (C), 137.1 (C), 132.4 (CH), 131.2 (CH), 129.3 (CH), 129.1 (q, $2J_{\text{C-F}} = 31.8$ Hz, C), 124.2 (q, $1J_{\text{C-F}} = 272.4$ Hz, C), 123.6 (q, $3J_{\text{C-F}} = 3.8$ Hz, 2CH), 114.3 (CH), 108.5 (CH), 52.2 (CH₂), 41.7 (CH₂). LC-MS (ESI+) Tr 5.07 min, m/z [M + H]⁺ 328.09. MW: 327.08 g·mol⁻¹. HRMS: m/z [M + H]⁺ calcd for [C₁₄H₁₂F₃N₃O₃]⁺: 328.0904; found: 328.0901.

N-(4-Bromophenyl)-2-(2-nitro-1*H*-pyrrol-1-yl)acetamide (16)

Yield 86% (291 mg). White solid. Mp 229–230 °C. ¹H NMR (400 MHz, DMSO-*d*₆) δ 10.52 (s, 1H, NH), 7.55–7.52 (m, 4H, 4CH), 7.35–7.34 (m, 1H, CH), 7.34–7.30 (m, 1H, CH), 6.32 (dd, $3J_{\text{H-H}} = 3.8$ Hz, $4J_{\text{H-H}} = 2.8$ Hz, 1H, CH), 5.24 (s, 2H, CH₂). ¹³C NMR (100 MHz, DMSO-*d*₆) δ 165.6 (C), 138.0 (C), 137.0 (C), 132.5 (CH), 131.7 (2CH), 121.0 (2CH), 115.1 (C), 114.1 (CH), 108.7 (CH), 52.8 (CH₂). LC-MS (ESI+) Tr 5.05 min, m/z [M + H]⁺ 323.98. MW: 322.99 g·mol⁻¹. HRMS: m/z [M + H]⁺ calcd for [C₁₂H₁₀BrN₃O₃]⁺: 323.9978; found: 323.9977.

N-(2-Chlorophenyl)-2-(2-nitro-1*H*-pyrrol-1-yl)acetamide (17)

Yield 96% (251 mg). White solid. Mp 178–179 °C. ¹H NMR (400 MHz, DMSO-*d*₆) δ 9.98 (s, 1H, NH), 7.68 (dd, $3J_{\text{H-H}} = 8.1$ Hz, $4J_{\text{H-H}} = 1.4$ Hz, 1H, CH), 7.51 (dd, $3J_{\text{H-H}} = 8.1$ Hz, $4J_{\text{H-H}} = 1.2$ Hz, 1H, CH), 7.39–7.37 (m, 1H, CH), 7.34–7.31 (m, 1H, CH), 7.28 (dd, $3J_{\text{H-H}} = 4.4$ Hz, $4J_{\text{H-H}} = 2.0$ Hz, 1H, CH), 7.22–7.18 (m, 1H, CH), 6.31 (dd, $3J_{\text{H-H}} = 4.4$ Hz, $4J_{\text{H-H}} = 2.7$ Hz, 1H, CH), 5.33 (s, 2H, CH₂). ¹³C NMR (100 MHz, DMSO-*d*₆) δ 166.1 (C), 137.0 (C), 134.4 (C), 132.4 (CH), 129.6 (CH), 127.5 (CH), 126.5 (CH), 126.2 (C), 125.9 (CH), 114.4 (CH), 108.6 (CH), 52.6 (CH₂). LC-MS (ESI+) Tr 4.44 min, m/z [M + H]⁺ 280.02. MW: 279.04 g·mol⁻¹. HRMS: m/z [M + H]⁺ calcd for [C₁₂H₁₀ClN₃O₃]⁺: 280.0483; found: 280.0483.

2-(2-Nitro-1*H*-pyrrol-1-yl)-*N*-[3-(trifluoromethyl)phenyl]acetamide (18)

Yield 81% (217 mg). White solid. Mp 202–203 °C. ¹H NMR (400 MHz, DMSO-*d*₆) δ 10.7 (s, 1H, NH), 8.06 (s, 1H, CH), 7.75–7.73 (m, 1H, CH), 7.55–7.59 (m, 1H, CH), 7.44–7.42 (m, 1H, CH), 7.37–7.35 (m, 1H, CH), 7.30 (dd, $3J_{\text{H-H}} = 4.3$ Hz, $4J_{\text{H-H}} = 2.1$ Hz, 1H, CH), 6.33 (dd, $3J_{\text{H-H}} = 4.4$ Hz, $4J_{\text{H-H}} = 2.7$ Hz, 1H, CH), 5.27 (s, 2H, CH₂). ¹³C NMR (100 MHz, DMSO-*d*₆) δ 166.1 (C), 139.4 (C), 137.0 (C), 132.5 (CH), 130.2 (CH), 129.5 (q, $2J_{\text{C-F}} = 32$ Hz, C), 124.0 (q, $1J_{\text{C-F}} = 271.0$ Hz, C), 122.6 (CH), 119.8 (q, $3J_{\text{C-F}} = 4.4$ Hz, CH), 115.0 (q, $3J_{\text{C-F}} = 3.6$ Hz, CH), 114.4 (CH), 108.7 (CH), 52.8 (CH₂). LC-MS (ESI+) Tr 5.21 min, m/z [M + H]⁺ 314.11. MW: 313.07 g·mol⁻¹. HRMS: m/z [M + H]⁺ calcd for [C₁₃H₁₀F₃N₃O₃]⁺: 314.0747; found: 314.0745.

N-(3-Methoxyphenyl)-2-(2-nitro-1*H*-pyrrol-1-yl)acetamide (**19**)

Yield 88% (217 mg). White solid. Mp 192–193 °C. ¹H NMR (400 MHz, DMSO-*d*₆) δ 10.39 (s, 1H, NH), 7.35–7.21 (m, 4H, 4CH), 7.08 (s, 1H, CH), 6.64 (s, 1H, CH), 6.32 (s, 1H, CH), 5.23 (s, 2H, CH₂), 3.72 (s, 3H, CH₃). ¹³C NMR (100 MHz, DMSO-*d*₆) δ 165.4 (C), 159.6 (C), 139.8 (C), 137.0 (C), 132.5 (CH), 129.7 (CH), 114.4 (CH), 111.2 (CH), 109.0 (CH), 108.6 (CH), 104.7 (CH), 54.9 (CH₃), 52.8 (CH₂). LC-MS (ESI+) Tr 4.32 min, *m/z* [M + H]⁺ 276.11. MW: 275.09 g·mol⁻¹. HRMS: *m/z* [M + H]⁺ calcd for [C₁₃H₁₃N₃O₄]⁺: 276.0979; found: 276.0979.

N-Isopropyl-2-(2-nitro-1*H*-pyrrol-1-yl)acetamide (**20**)

Yield 30% (57 mg). White solid. Mp 190–191 °C. ¹H NMR (400 MHz, DMSO-*d*₆) δ 8.09 (d, 3*J*_{H-H} = 7.5 Hz, 1H, NH), 7.27 (t, 3*J*_{H-H} = 2.4 Hz, 1H, CH), 7.22 (dd, 3*J*_{H-H} = 4.2 Hz, 4*J*_{H-H} = 2.1 Hz, 1H, CH), 6.25 (dd, 3*J*_{H-H} = 4.2 Hz, 4*J*_{H-H} = 2.7 Hz, 1H, CH), 4.95 (s, 2H, CH₂), 3.86–3.78 (m, 1H, CH), 1.07 (d, 3*J*_{H-H} = 6.6 Hz, 6H, 2CH₃). ¹³C NMR (100 MHz, DMSO-*d*₆) δ 165.3 (C), 137.1 (C), 132.3 (CH), 114.2 (CH), 108.3 (CH), 52.1 (CH), 40.7 (CH₂), 22.4 (2CH₃). LC-MS (ESI+) Tr 3.16 min, *m/z* [M + H]⁺ 212.34. MW: 211.10 g·mol⁻¹. HRMS: *m/z* [M + H]⁺ calcd for [C₉H₁₃N₃O₃]⁺: 212.1030; found: 212.1029.

N-Cyclopentyl-2-(2-nitro-1*H*-pyrrol-1-yl)acetamide (**21**)

Yield 59% (125 mg). White solid. Mp 190–191 °C. ¹H NMR (400 MHz, DMSO-*d*₆) δ 8.17 (d, 3*J*_{H-H} = 7.3 Hz, 1H, NH), 7.28 (t, 3*J*_{H-H} = 2.2 Hz, 1H, CH), 7.23 (dd, 3*J*_{H-H} = 4.2 Hz, 4*J*_{H-H} = 2.1 Hz, 1H, CH), 6.26 (dd, 3*J*_{H-H} = 4.4 Hz, 4*J*_{H-H} = 2.7 Hz, 1H, CH), 4.96 (s, 2H, CH₂), 4.01–3.96 (m, 1H, CH), 1.82–1.76 (m, 2H, CH₂), 1.67–1.64 (m, 2H, CH₂), 1.53–1.49 (m, 2H, CH₂), 1.44–1.37 (m, 2H, CH₂). ¹³C NMR (100 MHz, DMSO-*d*₆) δ 165.7 (C), 137.1 (C), 132.3 (CH), 114.2 (CH), 108.3 (CH), 52.1 (CH), 50.5 (CH₂), 32.3 (2 CH₂), 23.4 (2 CH₂). LC-MS (ESI+) Tr 3.85 min, *m/z* [M + H]⁺ 238.24. MW: 237.11 g·mol⁻¹. HRMS: *m/z* [M + H]⁺ calcd for [C₁₁H₁₅N₃O₃]⁺: 238.1186; found: 238.1191.

N-(2-Bromo-5-fluorophenyl)-2-(2-nitro-1*H*-pyrrol-1-yl)acetamide (**22**)

Yield 77% (123 mg). Yellow solid. Mp 185–186 °C. ¹H NMR (400 MHz, DMSO-*d*₆) δ 9.98 (s, 1H, NH), 7.75–7.71 (m, 1H, CH), 7.56–7.52 (m, 1H, CH), 7.07–7.02 (m, 1H, CH), 7.39 (t, 3*J*_{H-H} = 2.3 Hz, 1H, CH), 7.30 (dd, 3*J*_{H-H} = 4.4 Hz, 4*J*_{H-H} = 2.0 Hz, 1H, CH), 6.33 (dd, 3*J*_{H-H} = 4.4 Hz, 4*J*_{H-H} = 2.7 Hz, 1H, CH), 5.35 (s, 2H, CH₂). ¹³C NMR (100 MHz, DMSO-*d*₆) δ 166.4 (C), 161.0 (d, 1*J*_{C-F} = 241.2 Hz, C), 137.2 (C), 137.0 (d, 3*J*_{C-F} = 9.4 Hz, C), 134.0 (d, 3*J*_{C-F} = 9.4 Hz, CH), 132.4 (CH), 114.5 (CH), 113.8 (d, 2*J*_{C-F} = 22.5 Hz, CH), 112.6 (d, 2*J*_{C-F} = 26.1 Hz, CH), 110.9 (C), 108.7 (CH), 52.7 (CH₂). LC-MS (ESI+) Tr 4.84 min, *m/z* [M + H]⁺ 342.0. MW: 340.98 g·mol⁻¹. HRMS: *m/z* [M + H]⁺ calcd for [C₁₂H₉BrFN₃O₃]⁺: 341.9884; found: 341.9877.

3.1.5. Crystal Data for 2-Nitropyrrole Starting Product 1

Crystal Data for Compound 1 C₄H₄N₂O₂, M = 112.09, a = 7.7417(3) Å, b = 10.1820(5) Å, c = 21.2170(6) Å, α = 89.654(3)°, β = 89.210(3)°, γ = 69.065(4)°, V = 1507.42(11) Å³, T = 242 K, space group P1 Z = 12, 5673 independent reflections (R_{int} = 5673). The final R1 values were 0.0721 (I > 2σ(I)). The final wR(F 2) values were 0.1919 (I > 2σ(I)). The goodness of fit on F 2 was 1.159. CCDC 2132900 contains the supplementary crystallographic data for this paper. These data can be obtained free of charge at www.ccdc.cam.ac.uk/data_request/cif (accessed on 24 February 2022) or from the Cambridge Crystallographic Data Centre, 12, Union Road, Cambridge CB2 1EZ, UK; Fax: + 44 (1223) 336033; email: deposit@ccdc.cam.ac.uk.

3.2. Toxicology

The toxicity of compounds towards Chinese hamster ovary cells (CHO-K1, ATCC CCL61) was evaluated by the NRU toxicity test, based on the concentration-dependent reduction of the uptake of the vital dye neutral red when measured 24 h after chemical treatment. Cells were grown in McCoy's medium supplemented with Penicillin 100 IU/mL

and streptomycin 100 µg/mL, and 10% of inactivated calf serum, and incubated at 37 °C in CO₂ 5% atmosphere. They were seeded into two 96-well tissue culture plates (0.1 mL per well), at a concentration of 1 × 10⁵ cells/mL, and incubated at 37 °C (5% CO₂) for 24 h, until confluent. The culture medium was decanted and replaced by 100 µL of fresh medium containing the appropriate concentrations of the compounds (eight different concentrations in triplicate), then cells were incubated at 37 °C (5% CO₂) in the dark for 24 h. At the end of the incubation period, cells were washed, placed into neutral red medium (50 µg/mL neutral red in complete medium). This vital dye is a weak cationic dye that penetrates membranes of living cells by non-diffusion and accumulates intracellularly in lysosomes. On the contrary, alterations of the cell surface or metabolism result in a decreased uptake and binding of NR in non-viable cells. Cells were incubated for 3 h at 37 °C, 5% CO₂, and then the culture medium was removed, and cells were washed three times with 0.2 mL of PBS to remove excessive dye. Destaining solution (50% ethanol, 1% acetic acid, 49% distilled water; 50 µL per well) was added into the wells, and the plates were shaken for 15–20 min at room temperature in the dark. The degree of cell viability was measured by a fluorescence–luminescence reader. The optical density (OD) of each well was read at 540 nm. The results obtained for wells treated with the test compounds were compared to those of untreated control wells (100% viability) and converted to percentage values. The mean OD value of blank wells (containing only neutral red desorbed solution) was subtracted from the mean OD value of three treated wells (dilutions of the test material, positive control or HBSS). The percentages of cell viability were calculated as:

$$\text{Viability (\%)} = (\text{Mean OD of test wells} - \text{mean OD of blanks}) \times 100 / (\text{Mean OD of negative control} - \text{mean OD of blanks})$$

The concentration of the test substances causing a 50% release of neutral red as compared to the control culture was calculated by non-linear regression analysis using software Phototox Version 2.0.

3.3. *T. cruzi* Intracellular Assay

Vero cells (ECCAC 84113001) were screened for mycoplasma infection and maintained in MEM medium supplemented with Glutamax (Life Technologies) and 10% (*v/v*) foetal calf serum (FCS) at 37 °C in the presence of 5% CO₂. *T. cruzi* parasites (Silvio X10/7 A1), a clonal line kindly provided by Susan Wyllie and Prof. Alan Fairlamb were maintained in Vero cells. On a weekly basis, emerged trypomastigotes were used to infect a new Vero monolayer at the multiplicity of infection (MOI) 1.5 [32].

For the primary intracellular assay, the infection conditions were chosen so that no trypomastigote egress occurs during the compound incubation time. First, Vero cells were infected overnight with tissue culture-derived *T. cruzi* trypomastigotes in T225 tissue culture flasks (MOI 5).

Next, any remaining free trypomastigotes were washed away with serum-free MEM, and the infected Vero cells were harvested by trypsinisation. The infected Vero cells were then plated into 384-well plates containing the compounds to be tested, at 4000 cells per well in MEM media with 1% FCS. After 96h incubation at 37 °C in the presence of 5% CO₂, the plates were fixed with 4% formaldehyde for 20 min at room temperature and stained with 5 µg/mL Hoechst 33342. The plates were imaged on a Perkin Elmer Operetta high-content imaging system using a 20× objective. Images were analysed using the Columbus system (Perkin Elmer). The algorithm for the primary assay first identified the Vero nuclei followed by the demarcation of the cytoplasm and identification of intracellular amastigotes. This algorithm reported the mean number of parasites per Vero cell and the total number of Vero cells. The data analysis was as previously described [33].

The robust z-factor was calculated with the following formula:

$$1 - \frac{(3 \times (1.4826 \times \text{MAD}[0\% \text{ inhibition (raw data)}])) + (3 \times (1.4826 \times \text{MAD}[100\% \text{ inhibition (raw data)}]))}{\text{MEDIAN}[0\% \text{ inhibition (raw data)}] - \text{MEDIAN}[100\% \text{ inhibition (raw data)}]}$$

with MAD = Mean Absolute Deviation. Hits from the primary screen were selected based on the following criteria: *T. cruzi* activity (percent inhibition) > (median *T. cruzi* percent inhibition + 3 × robust Standard Deviation) and Vero activity (percent inhibition) < (median percent Vero inhibition + 3 × robust Standard Deviation).

4. Conclusions

A series of 10 novel 1-functionalized 2-nitropyrrole compounds were designed in accordance with Lipinski's rule of five, and synthesized with good yields. The convergent synthesis methodology allowed us to introduce in 1-position of the 2-nitropyrrole an acetamide side-chain close to that found in benznidazole by overcoming the pyrrole polymerization problem. The cytotoxicity evaluation on CHO cells showed no significant cytotoxicity, except for compound **3** (CC₅₀ < 30 µM). Compound **18** appeared to show that activity against *T. cruzi* intracellular amastigotes forms (EC₅₀ = 3.6 ± 1.8 µM) and good selectivity over the Vero host cells. Unfortunately, this compound **18** showed an insufficient maximum effect compared to the reference drug (nifurtimox) to ensure the further development of antichagasic compounds.

Supplementary Materials: The supporting information is available online at <https://www.mdpi.com/article/10.3390/molecules27072163/s1>: 1H- for intermediates compounds **5–13**; 1H and 13C-NMR for compounds **2–4** and **14–22**; dose-response curve data for EC₅₀ and CC₅₀ calculations of compounds **3, 4, 15, 16, 17** and **19**.

Author Contributions: Conceptualisation, F.M. and P.V.; methodology, F.M., Y.K. and D.B.; formal analysis, F.M., Y.K., D.B., C.D.G.; investigation, F.M., Y.K., D.B., C.D.G.; resources, P.V., C.D.G.; writing—original draft preparation, F.M., Y.K., D.B., C.D.G., P.V.; writing—review and editing, F.M., Y.K., D.B., N.P., C.D.G., P.V.; visualisation, F.M., Y.K., D.B., N.P., C.D.G., P.V.; supervision, P.V.; project administration, F.M., P.V. All authors have read and agreed to the published version of the manuscript.

Funding: This research received no external funding.

Institutional Review Board Statement: Not applicable.

Informed Consent Statement: Not applicable.

Data Availability Statement: Not applicable.

Acknowledgments: The authors would like to thank the Drug Discovery Unit at the University of Dundee for generating the *Trypanosoma cruzi* potency data. This work was supported by the CNRS (Centre National de la Recherche Scientifique) and Aix-Marseille Université. The authors thank V. Remusat for NMR spectra recording and the Spectropole team for various analytical measurements.

Conflicts of Interest: The authors declare no conflict of interest.

References

1. WHO | World Health Organization. Available online: <https://www.who.int/news/item/15-11-2021-who-and-bayer-renew-longstanding-collaboration-to-accelerate-control-and-elimination-of-neglected-tropical-diseases> (accessed on 22 January 2022).
2. Bonney, K.M.; Luthringer, D.J.; Kim, S.A.; Garg, N.J.; Engman, D.M. Pathology and Pathogenesis of Chagas Heart Disease. *Annu. Rev. Pathol.* **2019**, *14*, 421–447. [CrossRef] [PubMed]
3. Chagas Disease-PAHO/WHO | Pan American Health Organization. Available online: <https://www.paho.org/en/topics/chagas-disease> (accessed on 22 January 2022).
4. WHO Model Lists of Essential Medicines. Available online: <https://www.who.int/groups/expert-committee-on-selection-and-use-of-essential-medicines/essential-medicines-lists> (accessed on 22 January 2022).
5. Bern, C.; Montgomery, S.P.; Herwaldt, B.L.; Rassi, A.; Marin-Neto, J.A.; Dantas, R.O.; Maguire, J.H.; Acquatella, H.; Morillo, C.; Kirchhoff, L.V.; et al. Evaluation and Treatment of Chagas Disease in the United States: A Systematic Review. *JAMA* **2007**, *298*, 2171–2181. [CrossRef]
6. Kande Betu Ku Mesu, V.; Mutombo Kalonji, W.; Bardonneau, C.; Valverde Mordt, O.; Ngolo Tete, D.; Blesson, S.; Simon, F.; Delhomme, S.; Bernhard, S.; Mahenzi Mbembo, H.; et al. Oral Fexinidazole for Stage 1 or Early Stage 2 African Trypanosoma Brucei Gambiense Trypanosomiasis: A Prospective, Multicentre, Open-Label, Cohort Study. *Lancet Glob. Health* **2021**, *9*, 999–1008. [CrossRef]

7. Oral Fexinidazole Dosing Regimens for the Treatment of Adults With Chronic Indeterminate Chagas Disease-Full Text View-ClinicalTrials.gov. Available online: <https://clinicaltrials.gov/ct2/show/NCT03587766> (accessed on 22 January 2022).
8. Mazzeti, A.L.; Capelari-Oliveira, P.; Bahia, M.T.; Mosqueira, V.C.F. Review on Experimental Treatment Strategies Against *Trypanos. Cruzi*. *JEP* **2021**, *13*, 409–432. [[CrossRef](#)] [[PubMed](#)]
9. Primas, N.; Ducros, C.; Vanelle, P.; Verhaeghe, P. The Renewal of Interest in Nitroaromatic Drugs Towards New Anti-Kinetoplastid Agents. In *Medicinal Chemistry of Neglected and Tropical Diseases*; CRC Press: Boca Raton, FL, USA, 2019.
10. Russell, S.; Rahmani, R.; Jones, A.J.; Newson, H.L.; Neilde, K.; Cotillo, I.; Rahmani Khajouei, M.; Ferrins, L.; Qureishi, S.; Nguyen, N.; et al. Hit-to-Lead Optimization of a Novel Class of Potent, Broad-Spectrum Trypanosomacides. *J. Med. Chem.* **2016**, *59*, 9686–9720. [[CrossRef](#)]
11. Brand, S.; Ko, E.J.; Viayna, E.; Thompson, S.; Spinks, D.; Thomas, M.; Sandberg, L.; Francisco, A.F.; Jayawardhana, S.; Smith, V.C.; et al. Discovery and Optimization of 5-Amino-1,2,3-Triazole-4-Carboxamide Series against *Trypanos. Cruzi*. *J. Med. Chem.* **2017**, *60*, 7284–7299. [[CrossRef](#)]
12. Fersing, C.; Boudot, C.; Castera-Ducros, C.; Pinault, E.; Hutter, S.; Paoli-Lombardo, R.; Primas, N.; Pedron, J.; Seguy, L.; Bourgeade-Delmas, S.; et al. 8-Alkynyl-3-Nitroimidazopyridines Display Potent Antitrypanosomal Activity against Both *Trypanosoma brucei* and *Cruzi*. *Eur. J. Med. Chem.* **2020**, *202*, 112558. [[CrossRef](#)]
13. Saccoliti, F.; Madaia, V.N.; Tudino, V.; De Leo, A.; Pescatori, L.; Messori, A.; De Vita, D.; Scipione, L.; Brun, R.; Kaiser, M.; et al. Design, Synthesis, and Biological Evaluation of New 1-(Aryl-1*H*-Pyrrolyl)(Phenyl)methyl-1*H*-Imidazole Derivatives as Antiprotozoal Agents. *J. Med. Chem.* **2019**, *62*, 1330–1347. [[CrossRef](#)]
14. Hall, B.S.; Wilkinson, S.R. Activation of Benznidazole by Trypanosomal Type I Nitroreductases Results in Glyoxal Formation. *Antimicrob. Agents Chemother.* **2012**, *56*, 115–123. [[CrossRef](#)]
15. Hall, B.S.; Bot, C.; Wilkinson, S.R. Nifurtimox Activation by Trypanosomal Type I Nitroreductases Generates Cytotoxic Nitrile Metabolites. *J. Biol. Chem.* **2011**, *286*, 13088–13095. [[CrossRef](#)]
16. Kneeteman, M.; Baena, A.; Rosa, C.; Mancini, P. Polar Diels-Alder Reactions Using Heterocycles as Electrophiles. Influence of Microwave Irradiation. *IRJPAC* **2015**, *8*, 229–235. [[CrossRef](#)]
17. Cooksey, A.R.; Morgan, K.J.; Morrey, D.P. Nitropyrroles—II. *Tetrahedron* **1970**, *26*, 5101–5111. [[CrossRef](#)]
18. WO2017205622 Method of Making Benznidazole (wipo.int). Available online: <https://patentscope.wipo.int/search/en/detail.jsf?docId=WO2017205622> (accessed on 25 January 2022).
19. Allais, C.; Baslé, O.; Grassot, J.-M.; Fontaine, M.; Anguille, S.; Rodriguez, J.; Constantieux, T. Cooperative Heterogeneous Organocatalysis and Homogeneous Metal Catalysis for the One-Pot Regioselective Synthesis of 2-Pyridones. *Adv. Synth. Catal.* **2012**, *354*, 2084–2088. [[CrossRef](#)]
20. Tang, Z.; Li, X.; Yao, Y.; Qi, Y.; Wang, M.; Dai, N.; Wen, Y.; Wan, Y.; Peng, L. Design, Synthesis, Fungicidal Activity and Molecular Docking Studies of Novel 2-((2-Hydroxyphenyl)methylamino)Acetamide Derivatives. *Bioorg. Med. Chem.* **2019**, *27*, 2572–2578. [[CrossRef](#)]
21. Molinspiration Cheminformatics. Available online: <https://www.Molinspiration.com/> (accessed on 25 January 2022).
22. Lipinski, C.A.; Lombardo, F.; Dominy, B.W.; Feeney, P.J. Experimental and Computational Approaches to Estimate Solubility and Permeability in Drug Discovery and Development Settings. *Adv. Drug Deliv. Rev.* **2001**, *46*, 3–26. [[CrossRef](#)]
23. McKerrow, J.H.; Lipinski, C.A. The Rule of Five Should Not Impede Anti-Parasitic Drug Development. *Int. J. Parasitol. Drugs Drug. Resist.* **2017**, *7*, 248–249. [[CrossRef](#)] [[PubMed](#)]
24. Xie, H.; Ng, D.; Savinov, S.N.; Dey, B.; Kwong, P.D.; Wyatt, R.; Smith, A.B.; Hendrickson, W.A. Structure–Activity Relationships in the Binding of Chemically Derivatized CD4 to Gp120 from Human Immunodeficiency Virus. *J. Med. Chem.* **2007**, *50*, 4898–4908. [[CrossRef](#)] [[PubMed](#)]
25. Kushner, S.; Cassell, R.I.; Morton, J.; Williams, J.H. Anticonvulsants. *N*-Benzylamides. *J. Org. Chem.* **1951**, *16*, 1283–1288. [[CrossRef](#)]
26. Ferraccioli, R.; Forni, A. Selective Synthesis of Isoquinolin-3-One Derivatives Combining Pd-Catalysed Aromatic Alkylation/Vinylation with Addition Reactions: The Beneficial Effect of Water. *Eur. J. Org. Chem.* **2009**, *2009*, 3161–3166. [[CrossRef](#)]
27. Kadjane, P.; Platas-Iglesias, C.; Boehm-Sturm, P.; Truffault, V.; Hagberg, G.E.; Hoehn, M.; Logothetis, N.K.; Angelovski, G. Dual-Frequency Calcium-Responsive MRI Agents. *Chem. Eur. J.* **2014**, *20*, 7351–7362. [[CrossRef](#)]
28. Jogula, S.; Krishna, V.S.; Meda, N.; Balraju, V.; Sriram, D. Design, Synthesis and Biological Evaluation of Novel *Pseudomonas Aeruginosa* DNA Gyrase B Inhibitors. *Bioorg. Chem.* **2020**, *100*, 103905. [[CrossRef](#)] [[PubMed](#)]
29. Jiang, C.; Shi, J.; Liao, L.; Zhang, L.; Liu, J.; Wang, Y.; Lao, Y.; Zhang, J. 5-[2-(*N*-(Substituted Phenyl)Acetamide)]Amino-1,3,4-thiadiazole-2-sulfonamides as Selective Carbonic Anhydrase II Inhibitors with Neuroprotective Effects. *ChemMedChem* **2020**, *15*, 705–715. [[CrossRef](#)] [[PubMed](#)]
30. Samanta, S.; Lim, T.L.; Lam, Y. Synthesis and in Vitro Evaluation of West Nile Virus Protease Inhibitors Based on the 2-[6-[2-(5-Phenyl-4*H*-[1,2,4]Triazol-3-*Y*l)sulfanyl]Acetylaminol-Benzothiazol-2-*Y*l)sulfanyl]acetamide Scaffold. *ChemMedChem* **2013**, *8*, 994–1001. [[CrossRef](#)]
31. Lucas, R.L.; Zart, M.K.; Murkerjee, J.; Sorrell, T.N.; Powell, D.R.; Borovik, A.S. A Modular Approach toward Regulating the Secondary Coordination Sphere of Metal Ions: Differential Dioxxygen Activation Assisted by Intramolecular Hydrogen Bonds. *J. Am. Chem. Soc.* **2006**, *128*, 15476–15489. [[CrossRef](#)]

32. De Rycker, M.; Thomas, J.; Riley, J.; Brough, S.J.; Miles, T.J.; Gray, D.W. Identification of Trypanocidal Activity for Known Clinical Compounds Using a New *Trypanosoma Cruzi* Hit-Discovery Screening Cascade. *PLoS Negl. Trop. Dis.* **2016**, *10*, e0004584. [[CrossRef](#)] [[PubMed](#)]
33. De Rycker, M.; Hallyburton, I.; Thomas, J.; Campbell, L.; Wyllie, S.; Joshi, D.; Cameron, S.; Gilbert, I.H.; Wyatt, P.G.; Frearson, J.A.; et al. Comparison of a High-Throughput High-Content Intracellular Leishmania Donovanii Assay with an Axenic Amastigote Assay. *Antimicrob. Agents Chemother.* **2013**, *57*, 2913–2922. [[CrossRef](#)] [[PubMed](#)]